Numerically-Predicted Velocities of C_1 and C_2 Hydrofluorocarbon Refrigerant Flames with Air

Gregory LINTERIS*, Valeri BABUSHOK

Engineering Laboratory, National Institute of Standards and Technology
Gaithersburg, MD, USA
Phone: 301-975-2283, Email: linteris@nist.gov

* Corresponding Author

ABSTRACT

Due to their high global warming potentials, many existing working fluids for heating, cooling and refrigeration equipment are being phased out. Their replacements will often be flammable or slightly flammable, and the burning velocity of refrigerant-air mixtures is being used as a metric to rank their flammability. To allow industry to estimate the flammability of new blends of agents, predictive tools for the burning velocity of refrigerants are being developed, and calculating burning velocity requires a kinetic mechanism. The National Institute of Standards and Technology hydrofluorocarbon (HFC) mechanism was developed 20 years ago to describe hydrocarbon-air flames with added trace amounts of hydrofluorocarbon fire retardants (primarily CH_2F_2, CF_3H, CF_4, $C_2H_2F_4$, C_2HF_5, and C_2F_6). In the present work, the mechanism has been updated slightly to include new HFC compounds, more recent rate data, and rate data for new species. The modified mechanism is used to predict steady, planar, 1D, unstretched burning velocities for mixtures of air with each of the one- and two-carbon saturated HFC compounds R41 (CH_3F), R32 (CH_2F_2), R161 (C_2F_5H), R152 (CH_2F-CH_2F), R152a (CH_3-CHF_2), R143 (CH_2F-CHF_2), R143a (CH_3-CF_3), R134 (CHF_2-CHF_2), and R134a (CH_2F-CF_3), for which existing experimental data were available. Simulation results are present for a range of fuel-air equivalence ratio ϕ, for comparison with the available experimental data. Agreement is reasonable, and major kinetic pathways and radical populations are explored to uncover the general reaction properties of these new flames.

1. INTRODUCTION

Existing refrigerant working fluids in vapor-compression heating/cooling equipment that have high global warming potential (GWP)are being phased out through international treaties (i.e., the Kigali Agreement, an addendum to the Montreal Protocol.). Low-GWP replacements have been developed, primarily by adding double bonds or hydrogen atoms to the molecules, which makes them break down in the troposphere. Unfortunately, these properties also make them more flammable. Flammable refrigerants are a new challenge for the heating, ventilation, and air-conditioning and refrigeration industry, and new building standards are required for the safe use of the new compounds. Burning velocity has been adopted as part of the standard to characterize the new refrigerants. The laminar burning velocity is a useful parameter for quantifying fire risk since it is fundamental parameter that combines the effects of energy release, heat and mass transfer, and overall reaction rate. Moreover, predictions of turbulent flame speed are based on the laminar burning velocity, so the overpressure hazard and explosion hazard are both tied to the laminar burning velocity.

To meet the challenges of high efficiency, good volumetric capacity, low toxicity, zero ozone depletion potential, low GWP, and low flammability, industry will use blends of compounds. Analytical methods exist for optimizing the blends for all these properties except for flammability. To allow industry to estimate the flammability of new blends of agents, predictive tools for the burning velocity of refrigerants are being developed. Such a tool would help to accelerate the search for efficient blends that minimize the flammability hazard.

There are three parts to the development of the burning velocity predictive ability: 1.) understanding the experimental flame features so that the experimental burning velocity data can be accurately reduced and compared with the appropriate numerical simulation, 2.) applying and developing the necessary numerical simulation tools, and 3.) acquiring or developing the necessary input data to the models so that they can be implemented. The first two parts are dealt with in separate parts of the current project; the third part, obtaining the necessary input data, is the subject of the present manuscript. The necessary input parameters consist of: thermodynamic data (enthalpy and entropy as a function of temperature), transport data (Lennard-Jones parameters), and gas-phase reaction rate data (Arrhenius parameters; i.e., activation energy, pre-exponential, and pressure-dependency term) for all elementary reactions. In addition, the spectral radiation properties of the refrigerants and combustion products, as a function of temperature and pressure for the latter, will eventually be required to account for radiation heat losses in the flames.

As a starting point to obtain the necessary input kinetic parameters for flame modeling, an existing model for hydrofluorocarbon (HFC) flame behavior is adopted in the present work, and updated slightly. The National Institute of Standards and Technology (NIST) hydrofluorocarbon (HFC) mechanism (and its associated transport parameters) was developed 20 years ago to describe the addition of HFC fire suppressants to hydrocarbon-air flames. While some of the one-, two-, and three-carbon HFC compounds are the same as those being considered as refrigerants (as pure compounds or in blends), an assumption in the original model was that the HFC suppressant was added at small concentrations to stable hydrocarbon-air flames. Hence, the predominant species attacking the HFC reactants were the typical hydrocarbon radical pool species (H, O, and OH), and hydrocarbon radicals. For flames of pure refrigerants in air, however, the attack by fluorinated radicals is expected (Babushok *et al.*, 2012) and these reactions must be more thoroughly considered in the reaction set. The original NIST HFC mechanism is currently being updated and extended to apply to new refrigerants added at high concentrations in air, starting with R32 (Burgess Jr *et al.*, 2018), and will likely require additional reactions and species. As a first step in this process, however, the existing NIST HFC mechanism is applied to predict burning velocities of some pure C_1 and C_2 HFC compounds in air, and the results are compared to existing experimental data for burning velocity.

The NIST HFC mechanism was first tested with no modifications. Agreement was initially good for some compounds and poor for others. Consequently, some improvements were made, including addition of new HFC intermediates and their reactions, more recent rate data, and updated thermodynamic data, as described below. The modified mechanism is then used to predict steady, adiabatic, planar, 1D, unstretched burning velocities S_u^0 for mixtures of each refrigerant with air, over a range of fuel-air equivalence ratio ϕ, for comparison with experimental values in the literature. The compounds modeled are the saturated C_1 and C_2 HFC compounds R50 (CH_4), R41 (CH_3F), R32 (CH_2F_2), R170 (C_2H_6) R161 (C_2F_5H), R152 (CH_2F-CH_2F), R152a (CH_3-CHF_2), R143 (CH_2F-CHF_2), R143a (CH_3-CF_3), R134 (CHF_2-CHF_2), and R134a (CH_2F-CF_3), for which existing data were available.

2. KINETIC MODEL

The starting kinetic model is from the NIST C_1-C_2 HFC model (Burgess Jr *et al.*, 1995a, 1995b). That mechanism had subsequently been updated and expanded to include larger three-carbon HFC's (R-227ea) and other compounds, as described in (Babushok *et al.*, 2015), and to account for new reactions important for the combustion of pure fire suppressants (R23, R125, and R227ea) in air (Babushok *et al.*, 2012). Since the original work, a rather large amount of new kinetic data on the reactions of fluorine containing species has been published. Hence, the kinetic model has been updated to include some new species and recent reaction rate data. The thermodynamic data for fluorine-containing species in the mechanism haver also been updated using the data of Burcat and co-workers (Goos *et al.*, 2012). For the hydrocarbon sub-mechanism, GRIMech 2.11 (Frenklach *et al.*, 1995) was originally used, and this has been updated to GRIMech 3.0 (Smith *et al.*, 2000). The successive stages of the previously updated NIST HFC mechanism has been validated in numerous studies, comparing predicted and measured laminar burning velocities (Choi *et al.*, 2016; Linteris, 1996; Linteris *et al.*, 1998; Linteris and Truett, 1996; Pagliaro *et al.*, 2016a; Pagliaro *et al.*, 2016b), counterflow diffusion flame extinction conditions (Saso *et al.*, 2000), co-flow diffusion flame extinction conditions (Katta *et al.*, 2006; Takahashi *et al.*, 2015), and intermediate species profiles in low-pressure premixed flames (L'Esperance *et al.*, 1997; L'Esperance *et al.*, 1999; Williams *et al.*, 2000) and flow reactors (Takahashi *et al.*, 2007; Yu *et al.*, 2006).

Although they are not currently used in refrigerant blends, the mono-fluoro alkanes R41 (CH_3F) and R161 (CH_3-CH_2F) are included in the present study for completeness, and because experimental burning velocity data for them

are available. Although the compounds were present in the original HFC mechanism, they were not thoroughly treated there because they are not fire suppressants (they are highly flammable), and as trace intermediates in fire suppression studies they are present only at very low concentrations. Not surprisingly, for these two compounds, the predicted peak laminar burning velocity using the original HFC mechanism was in significant error (35 % low, and 22 % high, respectively) as compared to the experimental values. Hence, additions and changes were made to the NIST HFC mechanism to improve the agreement, including, for CH_3F, modifications to its heat of formation and to reactions of CH_2F with O_2.; and for C_2F_5H, modifications to the reaction rates (within their experimental uncertainty) of some of its initial decomposition products. The final mechanism used in the present work is referred to below as the updated NIST HFC mechanism, and it has 101 species and 915 reactions.

It should be noted that the present kinetic model should be considered as a starting point for further development and refinement. Numerous changes to both the rates and the reactions may be made once a variety of experimental data and theoretical results are available for testing the mechanism.

3. FLAME MODEL

The laminar burning velocities were calculated using the open-source Cantera software package (Goodwin *et al.*, 2016). The equations of mass, species, and energy conservation are solved numerically for the initial gas compositions, temperature (298 K), and pressure (101.33 kPa) corresponding to those in the experiments. The solution assumes isobaric, adiabatic, steady, planar, one-dimensional, laminar flow and neglects radiation and the Dufour effect, but includes thermal diffusion. Molecular diffusion is modeled with the multi-component transport equations. The boundary conditions, corresponding to a freely-propagating flame, are a fixed inlet temperature of 298 K and specified mass flux fractions at the inlet, and vanishing gradients downstream from the flame. The maximum gradient and curvature parameters in the simulation are selected to provide about 150 grid points in the solution, providing the unstretched laminar burning velocity that is grid independent.

4. EXPERIMENTAL DATA

The experimental burning velocity data for the comparisons are from Takizawa and co-workers. For all of the refrigerants, the following experimental arrangement was used, and for some of the refrigerants, additional experiments were conducted. In the first, an electrical spark ignited the premixed fuel and air in a constant volume spherical vessel (3.05 L volume), and a dynamic pressure transducer recorded the pressure rise (Takizawa *et al.*, 2005, 2006). Using the pressure vs. time data, a two-zone thermodynamic model of the burned and unburned gases yielded the burning velocity as a function of temperature and pressure, and curve fits to that surface were used to extrapolate to room temperature conditions (298 K, 101.33 kPa), for which the data are presented. The curve fit parameters are also presented in the references, so experimentally-derived burning velocity data at other pressures and temperatures can be extracted.

For R32, R143, R143a, and R152a, experiments were also conducted in a cylindrical vessel (volume of 3.92 L) with optical access at the ends, which allowed schlieren imaging of the flame (Takizawa *et al.*, 2005). A high-speed camera recorded the increase in flame radius with time (defined as the burned gas burning velocity), and multiplying this by the density ratio of burned and unburned gases (calculated by assuming chemical equilibrium) produced the burning velocity relative to the unburned gases.

For R32, several other experiments were also used. The constant volume, pressure rise method was used with a slightly different chamber (cylindrical, volume 2.92 L), and experiments using this chamber were conducted under both normal gravity (1g) and microgravity (0g) conditions (Takizawa *et al.*, 2013).

5. RESULTS AND DISCUSSION

Figure 1 and Figure 2 show, for a range of fuel-air equivalence ratios (ϕ), the adiabatic flame temperature T_{ad} (upper curves), and the laminar burning velocities S_u^0 (lower curves) calculated with Cantera. The figures also show the experimental data (points) of Takizawa and co-workers from outwardly propagating spherical flames in constant volume and constant pressure experiments (Takizawa *et al.*, 2013; Takizawa *et al.*, 2005, 2006). In Figure 1 and Figure 2, the open symbols denote experiments in the constant volume apparatus in which pressure rise is measured

(Takizawa *et al.*, 2005, 2006) in 1g, while the closed circles in Figure 1 are for the same experiment in 0g (R32 only). The crosses (in both Figure 1 and Figure 2) denote results from experiments in the constant pressure device using schlieren imaging of the flame growth (Takizawa *et al.*, 2013). Although no experimental data are available for pure R134a- or R134-air flames, the laminar burning velocities were calculated for illustration purposes. Table 1 summarizes the peak T_{ad} and S_u^0 from the experiments and simulations for each compound. Also shown are the stoichiometric volume fraction of each compound and the ratio of fluorine to hydrogen atoms in the original mixture, expressed as F/(F+H).

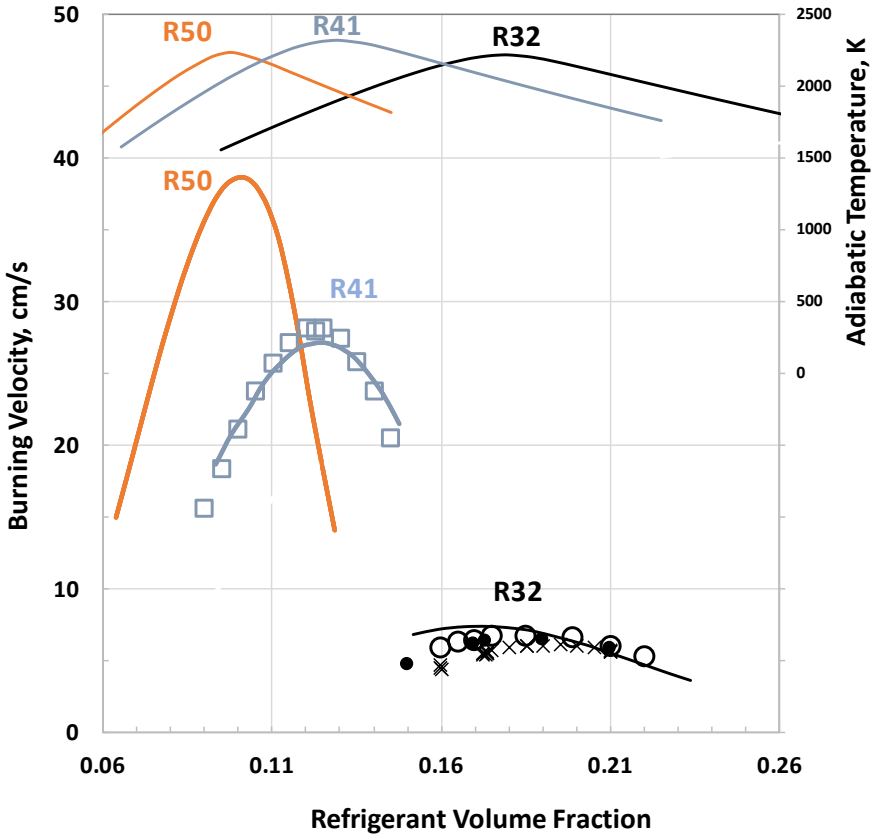

Figure 1: Burning velocity (left scale) and adiabatic flame temperature (right) for C_1 hydrofluorocarbons in air.

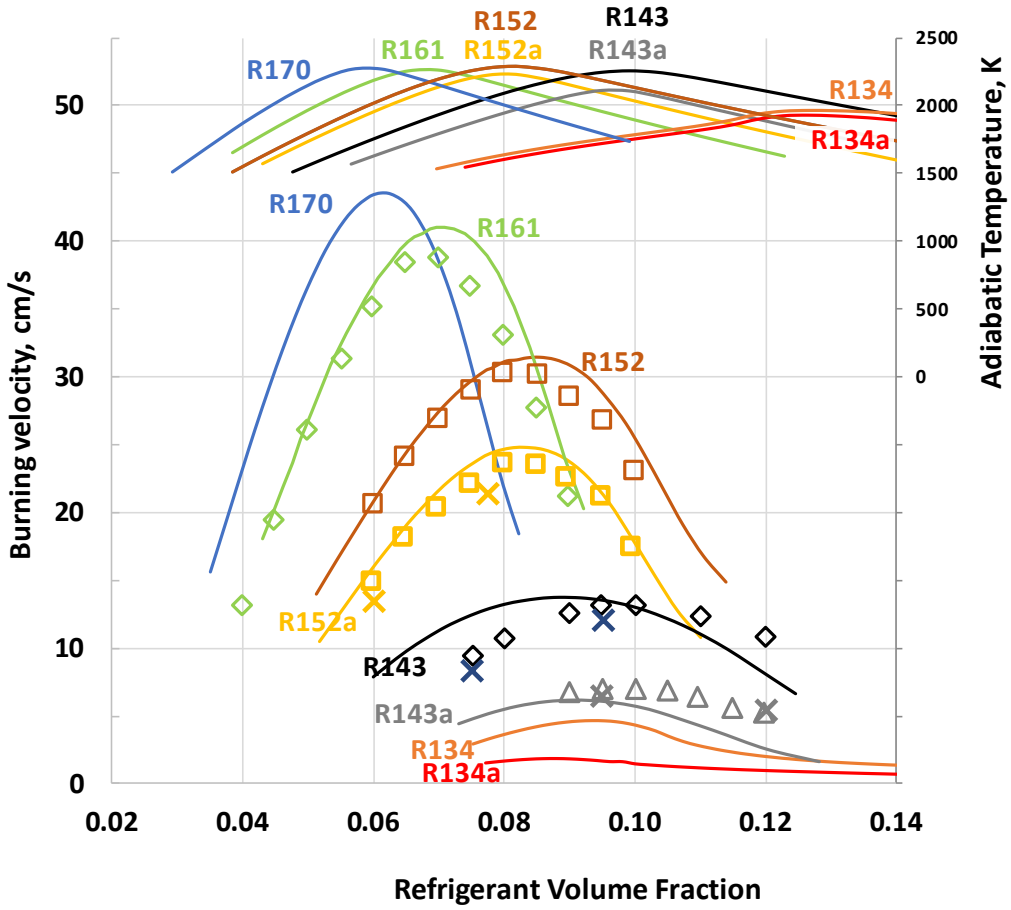

Figure 2: Burning velocity (left scale) and adiabatic flame temperature (right) for C_2 hydrofluorocarbons in air.

The stoichiometric concentration of the agents is generally higher than that for hydrocarbons, and increases as the fluorine loading in the molecule increases. The maximum T_{ad} are similar for the flammable HFCs (R161, R41, R152, R152a, R143, R143a), with the peak value in the range 2100 K <= T_{ad} <= 2300 K, which is comparable to, sometimes higher than, that of hydrocarbons. For the non-flammable refrigerants (R23, R134a, R134, and R125), the peak T_{ad} is somewhat lower (< 1960 K). As illustrated, the agreement in the measured and predicted burning velocity is reasonable for most refrigerants. For R143 and R143a, the simulations predict the peak burning velocity fairly well, although they show a peak value at leaner values of ϕ than measured in the experiments. It should be noted that agreement between predictions and measurements for the mono-fluoro compounds fluoromethane (CH_3F) and fluoroethane (C_2H_5F) using the original NIST model was poor. Modification of the enthalpy of formation for these compounds and kinetic data for several reactions was required to improve the predictions. Nonetheless, it should also be noted that stretch and burned gas thermal radiation have not yet been included in the simulations or in the reduction of the experimental data, and these might affect the results (Burrell *et al.*, 2018; Pagliaro and Linteris, 2016).

In Table 1, burning velocities and adiabatic flame temperatures are listed from highest value of S_u^0 to lowest; both T_{ad} and S_u^0 decrease with increasing fluorine loading in the refrigerant. This is also shown in Figure 3, which presents T_{ad} (Δ symbols) and S_u^0 (• symbols) as a function of the fluorine loading the system. As indicated, the asymmetrical isomers tend to be less flammable than the symmetrical ones, having both lower T_{ad} and S_u^0.

Table 1: Burning velocities and adiabatic combustion temperatures for stoichiometric refrigerant-air mixtures (initial temperature 298 K, 1 bar).

Refrigerant	Formula	T_{ad} K	S_u^0 max (Expt.) cm/s	S_u^0 max (Calc.) cm/s	$X_{stoic.}$ %	F/(F+H)
Flammable:						
R-170	C_2H_6	2265	40.9	43.1	5.66	0.00
R161	C_2H_5F	2265	38.3	41	6.54	0.17
R-50	CH_4	2230	36.5	38.6	9.5	0.00
R-152	CH_2F-CH_2F	2278	30.1	32.1	7.75	0.33
R-41	CH_3F	2273	28.3	27.2	12.3	0.25
R-152a	CH_3-CHF_2	2227	23.6	24.9	7.75	0.33
R-143	CH_2F-CHF_2	2248	13.1	13.7	9.5	0.50
R-32	CH_2F_2	2207	6.7	7.3	17.4	0.50
R-143a	CH_3-CF_3	2115	7.1	6.1	9.5	0.50
Non-Flammable:						
R-134	CHF_2-CHF_2	1958		4.6	12.3	0.67
R134a	CH_2F-CF_3	1931		1.8	12.3	0.67
R-125	CHF_2-CF_3	1793		1.56 (at 400K)	17.4	0.83
R-23	CHF_3	1713		0.57 (at 400K)	29.6	0.75
R-116	C2F6	1389		0	29.58	1.00

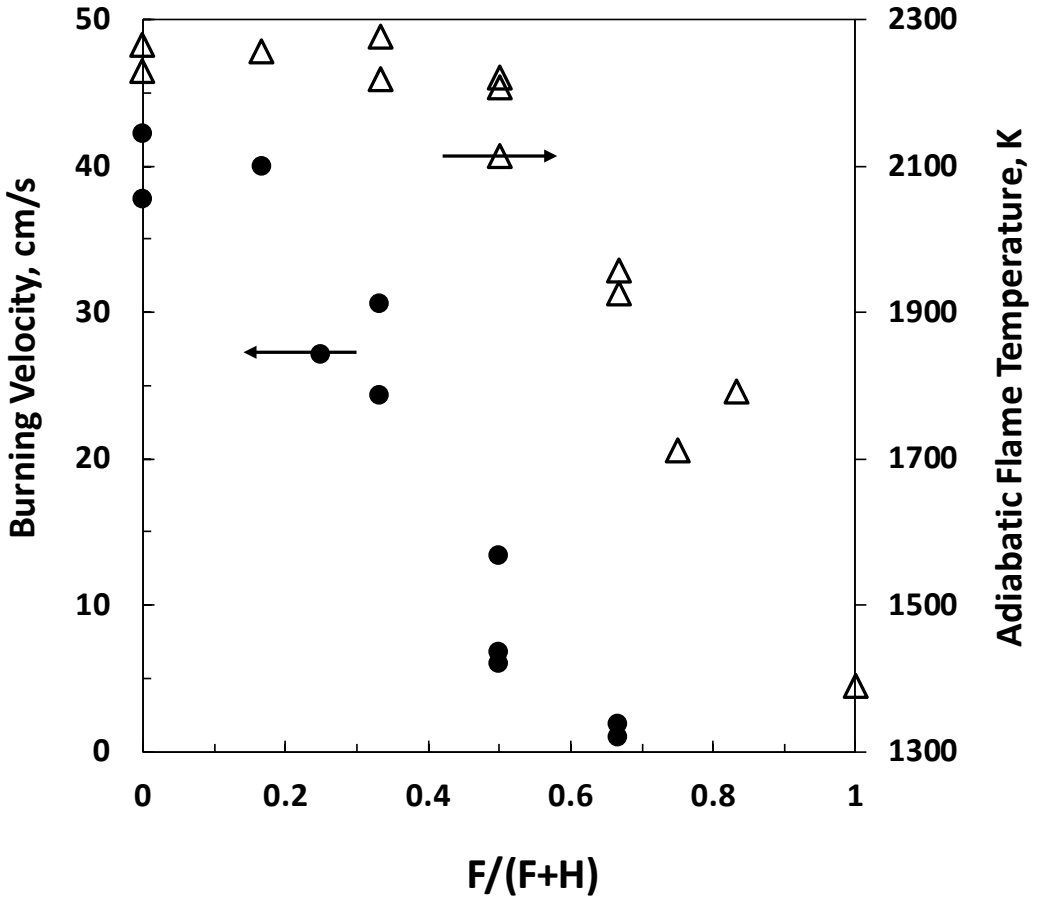

Figure 3: Burning velocity (•, left scale) and adiabatic flame temperature (Δ, right scale) as a function of the ratio of F atoms to F plus H atoms in the initial refrigerant-air mixture.

Using the calculated flame structures, the variation in radical concentrations with fluorine loading is determined. The peak volume fraction of chain-carrying radicals (H, O, and OH) is typically near the point of peak heat release in the flame, or the location reaching approximately 95 % of the peak flame temperature. Figure 4 (note semi-log plot) shows the sum of the peak volume fraction of chain-carrying radicals (H, O, and OH) and of F-containing radicals (at location of peak [OH]), as a function of the fluorine loading. As illustrated, the former drops off rapidly as the number of H atoms in the system becomes close to that of F atoms F/(F+H)=0.5, while the F radicals increase rapidly. Hence, at higher fluorine loading, the chemistry becomes dominated by fluorine-containing radicals. Figure 5 shows that with increased fluorine loading, the volume fraction of both F-atoms (at the point of maximum OH volume fraction) and sum of the peak for F-containing radicals increases steadily, as does the equilibrium F atom volume fraction, which becomes higher than the value in the flame zone. For these flames equilibrium F atom volume fraction (far downstream in the calculation domain) can be on the order of 1 %.

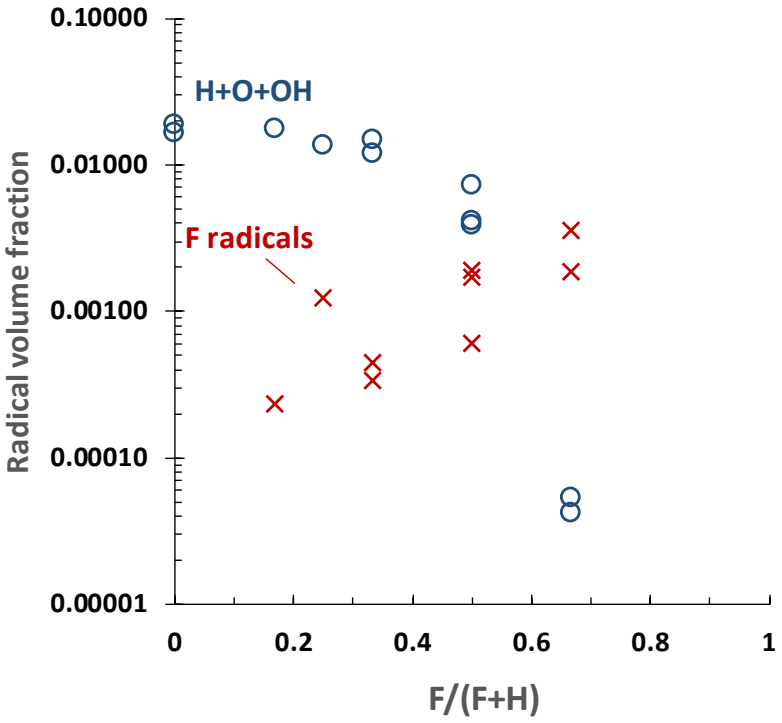

Figure 4: Volume fraction of total chain-branching radicals (H+O+OH) and F atoms in the flame reaction zone (i.e., the point of peak [OH]) as a function of the ratio of fluorine loading.

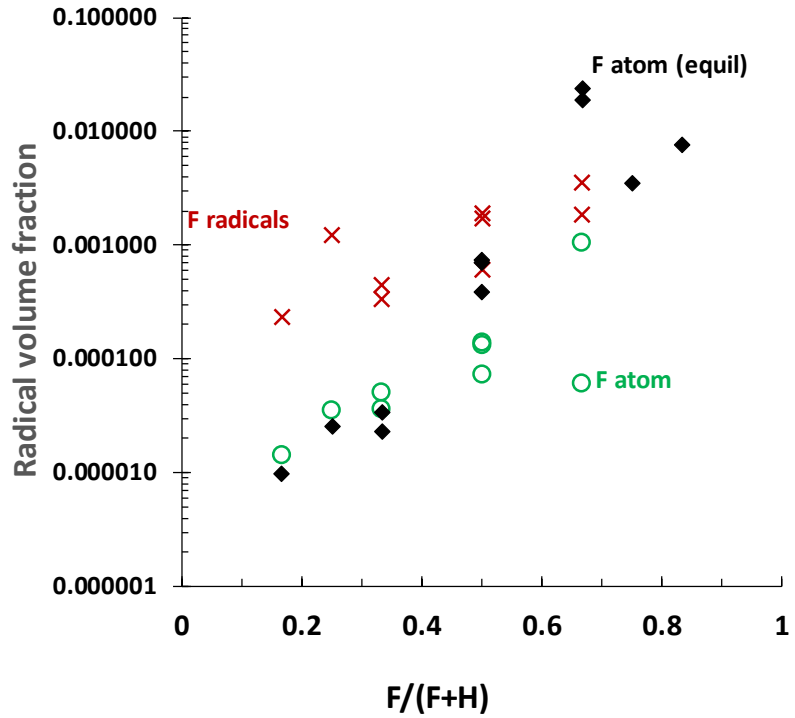

Figure 5: Volume fraction for fluorine radicals (F-radicals) and F atoms in the flame reaction zone, and for F atoms at equilibrium as a function fluorine loading.

6. CONCLUSIONS

The unstretched, laminar, planar, 1D, adiabatic burning velocities of saturated C_1 and C_2 HFC refrigerants (R41, R32, R161, R152, R152a, R143, R143a, R134, R134a were calculated using the original NIST HFC mechanism available in the literature and compared to existing experimental data. The predictions, for a range of fuel-air equivalence ratios, were in significant disagreement for CH_3F and C_2H_5F, and mild disagreement for other compounds. Consequently, the NIST HFC mechanism was modified with additional reactions, using more recent rate data in the literature, and with updated thermodynamic properties. After the changes, the agreement for these refrigerants is reasonable.

The mechanism is then used to examine the properties of the refrigerant-air flames. Adiabatic temperatures of the flammable refrigerant-air flames are comparable to, and sometimes higher than, similar hydrocarbons, whereas T_{ad} of the non-flammable refrigerants is lower. Burning velocity and flame temperature decrease as the fluorine to hydrogen ratio in the reactants increase. The symmetrical isomers of the fluoroethanes (R152, R143, R134) have higher adiabatic flame temperature and laminar burning velocity than the asymmetrical isomers (R152a, R143a, R134a). Analysis of the flame structures revealed that with increasing fluorine to hydrogen ratio, the chain-branching radical concentrations in the flame decrease, and fluorine-containing radicals, particularly F atom, increase. At high enough F/H ratio, the F atom equilibrium values are even higher than those in the flame zone.

While agreement between measured and predicted burning velocities is reasonable using the updated mechanism, work should be done to update and improve the kinetic mechanism. Also, flame stretch and radiation have not been included in either reduction of the experimental data or in the flame modeling, and these should be included in future work to increase the accuracy.

REFERENCES

Babushok, V. I., Linteris, G. T., Burgess, D. R., & Baker, P. T. (2015). Hydrocarbon flame inhibition by C3H2F3Br (2-BTP). *Combust. Flame, 162*(4), 1104-1112.

Babushok, V. I., Linteris, G. T., & Meier, O. (2012). Combustion properties of halogenated fire suppressants. *Combust Flame, 159*, 3569-3575.

Burgess Jr, D. R., Manion, J. A., Burrell, R., Babushok, V. I., Hegetschweiler, M. J., & Linteris, G. T. (2018). Development and validation of a mechanism for flame propagation in R-32/air mixtures. *2018 Eastern States Section Meeting of the Combustion Institute* State College, PA: The Combustion Institute

Burgess Jr, D. R., Zachariah, M. R., Tsang, W., & Westmoreland, P. R. (1995a). Thermochemical and chemical kinetic data for fluorinated hydrocarbons. *Prog. Energy Combust. Sci., 21*(6), 453-529.

Burgess Jr, D. R., Zachariah, M. R., Tsang, W., & Westmoreland, P. R. (1995b). *Thermochemical and Chemical Kinetic Data for Fluorinated Hydrocarbons*. (NIST Technical Note 1412). Gaithersburg, MD: National Institute of Standards and Technology.

Burrell, R., Pagliaro, J. L., & Linteris, G. T. (2018). Effects of stretch and thermal radiation on difluoromethane-air burning velocity measurements in constant volume spherically expanding flames. *Proc. Combust. Inst., 37*, submitted.

Choi, B. C., Park, J. S., & Ghoniem, A. F. (2016). Characteristics of outwardly propagating spherical flames of R134a(C2H2F4)/CH4/O-2/N-2 mixtures in a constant volume combustion chamber. *Energy, 95*, 517-527.

Frenklach, M., Wang, H., Yu, C.-L., Goldenberg, M., Bowman, C. T., Hanson, R. K., Davidson, D. F., Chang, E. J., Smith, G. P., Golden, D. M., Gardiner, W. C., & Lissianski, V. (1995). *GRI-mech: an optimized detailed chemical reaction mechanism for methane combustion*. (Gas Research Institute Topical Report No. GRI-95/0058, http://www.me.berkeley.edu/gri_mech). Chicago, IL.

Goodwin, D. G., Moffat, H. K., & Speth, R. L. (2016). *Cantera: An object-oriented software toolkit for chemical kinetics, thermodynamics, and transport processes. Version 2.1.1*. Pasedena, CA: California Institute of Technology, Retrieved from http://www.cantera.org.

Goos, E., Burcat, A., & Ruscic, B. (2012). Extended third millennium thermodynamic database for combustion and air-pollution use with updates from active thermochemical tables. Retrieved from Ftp://ftp.technion.ac.il/pub/supported/aetdd/thermodynamics/BURCAT.THR

Katta, V. R., Takahashi, F., & Linteris, G. T. (2006). Fire-suppression characteristics of CF_3H in a cup burner. *Combust. Flame, 144*(4), 645-661.

L'Esperance, D., Williams, B. A., & Fleming, J. W. (1997). Detection of fluorocarbon intermediates in low-pressure premixed flames by laser-induced fluorescence. *Chemical Physics Letters, 280*(1-2), 113-118.

L'Esperance, D., Williams, B. A., & Fleming, J. W. (1999). Intermediate species profiles in low pressure premixed flames inhibited by fluoromethanes. *Combust. Flame, 117*(4), 709-731.

Linteris, G. T. (1996). Numerically Predicted Structure and Burning Velocity of Premixed CO-Ar-O_2-H_2 Flames Inhibited by CF_3H. *Combust. Flame, 107*(1-2), 72-84.

Linteris, G. T., Burgess, D. R., Babushok, V., Zachariah, M., Tsang, W., & Westmoreland, P. (1998). Inhibition of premixed methane-air flames by fluoroethanes and fluoropropanes. *Combust. Flame, 113*(1-2), 164-180.

Linteris, G. T., & Truett, L. (1996). Inhibition of premixed methane-air flames by fluoromethanes. *Combust. Flame, 105*(1-2), 15-27.

Pagliaro, J. L., Bouvet, N., & Linteris, G. T. (2016a). Premixed flame inhibition by CF3Br and C3H2F3Br (2-BTP). *Combust. Flame, 169*, 272-286.

Pagliaro, J. L., & Linteris, G. T. (2016). Burning velocities of marginally flammable refrigerant-air mixtures. *2016 Eastern States Section Meeting of the Combustion Institute* Princeton, NJ: The Combustion Institute

Pagliaro, J. L., Linteris, G. T., & Babushok, V. I. (2016b). Premixed flame inhibition by C2HF3Cl2 and C2HF5. *Combust. Flame, 163*, 54-65.

Saso, Y., Joboji, H., Koda, S., Saito, N., & Nishioka, M. (2000). Response of counterflow diffusion flame stabilized on a methanol pool to suppressant doping. *Proc. Combust. Inst., 28*, 2947-2955.

Smith, G. P., Golden, D. M., Frenklach, M., Moriarty, N. W., Eiteneer, B., Goldenberg, M., Bowman, C. T., Hanson, R. K., Song, S., Gardiner, J. W. C., Lissianski, V. V., & Qin, Z. (2000). GRI Mech 3.0. Retrieved from http://www.me.berkeley.edu/gri_mech

Takahashi, F., Katta, V. R., Linteris, G. T., & Babushok, V. I. (2015). Combustion inhibition and enhancement of cup-burner flames by CF3Br, C2HF5, C2HF3Cl2, and C3H2F3Br. *Proc. Combust. Inst., 35*, 2741-2748.

Takahashi, K., Harada, A., Horigome, S., Cho, R., & Inomata, T. (2007). Thermal decompositons of 1,1,1-trifluoroethane and pentafluoroethane in a turbulent flow reactor. *Combust. Sci. Technol., 179*(7), 1417-1432.

Takizawa, K., Takagi, S., Tokuhashi, K., Kondo, S., Mamiya, M., & Nagai, H. (2013). Assessment of Burning Velocity Test Methods for Mildly Flammable Refrigerants, Part 1: Closed-Vessel Method. *ASHRAE Trans., 119*(2), 243-254.

Takizawa, K., Takahashi, A., Tokuhashi, K., Kondo, S., & Sekiya, A. (2005). Burning velocity measurement of fluorinated compounds by the spherical-vessel method. *Combust. Flame, 141*(3), 298-307.

Takizawa, K., Takahashi, A., Tokuhashi, K., Kondo, S., & Sekiya, A. (2006). Burning velocity measurement of HFC-41, HFC-152, and HFC-161 by the spherical-vessel method. *J Fluorine Chem, 127*(12), 1547-1553.

Williams, B. A., L'Esperance, D. M., & Fleming, J. W. (2000). Intermediate species profiles in low-pressure methane/oxygen flames inhibited by 2-H heptafluoropropane: Comparison of experimental data with kinetic modeling. *Combust. Flame, 120*(1-2), 160-172.

Yu, H., Kennedy, E. M., Mackie, J. C., & Dlugogorski, B. Z. (2006). An experimental and kinetic modeling study of the reaction of CHF3 with methane. *Environmental Science & Technology, 40*(18), 5778-5785.

ACKNOWLEDGEMENT

This work was supported by the Buildings Technologies Office of the U.S. Department of Energy, Office of Energy Efficiency and Renewable Energy under contract no. DE-EE0007615 with Antonio Bouza serving as Project Manager.